

# ATMOSPHERIC DYNAMICS OF THE JOVIAN LIKE PLANETS EPSILON ERIDANI b AND 55 CANCRI d

A. Sánchez-Lavega<sup>(1)</sup>, R. Hueso<sup>(1)</sup>, S. Baeza<sup>(2)</sup>

(1) *Dpto. Física Aplicada I, Escuela Superior de Ingenieros, Universidad del País Vasco, Bilbao (Spain). e-mail: wupsalaa@bi.ehu.es*

(2) *Dpto. Física Aplicada I, E.U.I.T.I., Universidad del País Vasco, Bilbao (Spain)*

## ABSTRACT

Epsilon Eridani b and 55 Cancr d are at present, the two extrasolar planets candidates with the largest orbital period and larger angular separation from its star. Their future detection depends on their albedo, and thus on cloud formation and dynamics. We present in this communication a first attempt to characterize their atmospheric circulation on the basis of the best observational available data and on a scale analysis for regular conditions in giant planets. The main basic unknown in this study is the planetary rotational (spin) period. We present different approaches to constraint it that suggests that the expected periods are in the range of those of Jupiter and Saturn. In such a case the usual geostrophic approach for atmospheric motions is expected, with a planetary regime dominated by zonal (East-West) jets. The most interesting case is that of Epsilon Eridani b whose high eccentricity, possible water clouds, and relatively short radiative time constant, could produce large-scale disturbances and profound changes in its dynamical regime along the seasonal cycle. No massive upper clouds are expected for 55 Cnc d, that probably is a very different gaseous planet. We discuss the range of plausible values for the spatial and temporal scales of motions.

## 1. INTRODUCTION

Because of their proximity to Earth and large angular separation from their stars, the planets Epsilon Eridani b and 55 Cancr d are enticing candidates for first direct detection with planned space missions and ground-based interferometric techniques. 55 Cnc d reaches an angular separation of  $\sim 0.45$  arcsec and Epsilon Eridani b  $\sim 1$  arcsec, but their detection will depend on their albedo (controlled by temperature and cloud formation), and thus on their atmospheric dynamics. These planets are also interesting because they are among the best characterized of the more than one hundred so far discovered. In addition, they probably differ markedly in mass and age, which in turn are different from that of Jupiter, so both serve to explore the variety of plausible dynamical regimes operating in the atmospheres of the giant planets. In this paper we analyze what kind of

motions can be expected in the atmospheres of these bodies. A first major problem is that the rotational period is unknown. In fact a constraint to it should come from future direct photometric observations. A second major problem is that current models of the general circulation of the Jovian-planets are very rudimentary [1]. For example the depth to which the winds extend, or the energy source that drives them, or how the strong eastward equatorial jets are generated, are still unexplained. Thus studies on the atmospheric dynamics of extrasolar planets should be considered at the exploratory level and useful for a first look to their influence on temperature and cloud distribution. In previous papers [2-3], we have performed a broad analysis of giant planets dynamical regimes based on a similarity scale analysis of the main parameters that control the atmospheric dynamics. Other authors have given a further step, exploring with more detail (including numerical simulations) the circulation of the so-called “hot Jupiters”, since for these cases the rotation period is expected to be the orbital period due to spin-orbit synchronization [4-6]. Here we concentrate on the other extreme group of planets so far discovered, those that are far away from their star. We focus our previous work (similarity, scale analysis) in the two bodies that pertain to a class somewhat between the “hot Jupiter” cases and our own Solar System cold Jupiter – Saturn planets.

## 2. OBSERVATIONAL DATA FOR $\epsilon$ Eridani b AND 55 Cnc d

In Tables 1 and 2 we summarize the measured and derived basic properties for the stars  $\epsilon$  Eridani and 55 Cancr and their planets b and d respectively [7-9]. One important property not constrained from radial velocity measurements is the mass. However,  $\epsilon$  Eri has a dust disk and so we assume the planet to be in the orbital plane of the disk (tilt  $\sim 25^\circ$ ) [7]. This is also compatible with one astrometric measurement that give for  $\epsilon$  Eri b a mass  $M_p = 1.2 \pm 0.33 M_J$  [10]. The star 55 Cnc is suspected to have also a disk, although it remains controversial [7]. It is a visual binary separated from the primary by a distance of 1100 a.u. [7]. We assume 55

Cnc d to be also in the suspected plane of this disk. Thus the actual mass for both planets is calculated using these orbital tilt angles.

Star	d (pc)	Separation	Spect. Type	Age (Gy)	$L_*$ ( $L_\odot$ )	$T_{\text{eff}}$ (K)	M ( $M_\odot$ )
$\epsilon$ Eri	3.2	1.0 arcsec	K2V	0.5-2	0.35	5150	0.81
55 Cnc	12.5	0.47 arcsec	G8V	3-8	0.61	5200	0.95

Table 1. Star Data

Planet	a	Period	e	$M_p \sin i$	i	$M_p$
$\epsilon$ Eri b	3.3	6.85	0.608	0.86	25°	2
55 Cnc d	5.9	14.7	0.16	4	27°	9

Table 2. Planet Data.

### 3. ENERGY SOURCES

In Table 3 we present the values for the orbital average of the incoming stellar energy flux on each planet  $\langle F_* \rangle$  ( $\text{W/m}^2$ ), albedo  $A$  (for  $\epsilon$  Eri b the albedo depends strongly on water cloud formation, see below) [11], the absorbed energy flux in the atmosphere  $F_{\text{abs}}$  ( $\text{W/m}^2$ ), and the internal energy flux  $F_{\text{int}}$  ( $\text{W/m}^2$ ) which is derived from evolutionary models [12] based on the star age. In the case of planets with a large orbital eccentricity, an average value for the stellar energy flux can be obtained as follows

$$\langle F_* \rangle = \frac{L_*}{4pa^2(1-e^2)^{1/2}} \quad (1)$$

Here  $L_*$  is the stellar luminosity,  $a$  is the semi-major axis and  $e$  the eccentricity. The effective temperature ( $T_{\text{eff}}$ ) and equilibrium temperature ( $T_{\text{eq}}$ ) are then calculated (in degrees Kelvin). See e.g. ref. [2] for definitions of all these magnitudes. A range of values is given for  $\epsilon$  Eri b according to the expected albedo range. Finally, a fundamental parameter for atmospheric dynamics, “the energy balance” (averaged during the orbital cycle) is then calculated by

$$\langle E \rangle = \frac{F_{\text{abs}} + F_{\text{int}}}{F_{\text{abs}}} = \left( \frac{T_{\text{eff}}}{T_{\text{eq}}} \right)^4 \quad (2)$$

For  $\langle E \rangle = 1$ , the stellar (external) insolation dominates. For  $\langle E \rangle > 1$ , the internal source is expected to increase its dominance as  $\langle E \rangle$  increases.

Planet	$\langle F_* \rangle$	A	$F_{\text{abs}}$	$T_{\text{eq}}$	$F_{\text{int}}$	$T_{\text{eff}}$	$\langle E \rangle$
$\epsilon$ Eri b	44.3	0.4 – 0.8	7-2	104-79	40	169-165	7-19
55 Cnc d	24.5	0.13	3.7	90	497	306	134
Jupiter	51	0.343	8.1	109	5.4	124	1.67

Table 3. Energy Sources.

Obviously, strong seasonal changes, that affect the absorbed stellar flux, are expected in  $\epsilon$  Eri b due to the large orbital eccentricity. This will be discussed in section 7.

### 4. VERTICAL STRUCTURE

Both planets are assumed to be “Jovian-like” in composition (mean molecular weight  $m = 2.12 \text{ g mol}^{-1}$ ). The radius is obtained from the evolutionary models of isolated planets as derived from the age of the star [12] and expressed in terms of the Jovian radius ( $R_J = 71400 \text{ km}$ ). The atmosphere depth, i. e. the vertical extent  $D$  of the  $\text{H}_2$  layer (given in planetary radius fraction) is determined from an interior model of the planets that uses as the state equation a polytrope ( $P = K \rho^2$ , with  $P$  the pressure,  $\rho$  the density and  $K = 2GR_p/p$ ), and assuming that the transition from the  $\text{H}_2$  fluid layer to  $\text{H}^+$  (fluid metallic, the base of the atmosphere) takes place at a pressure  $P \sim 2 \text{ Mbar}$  [13]. At this level we get a temperature of  $\sim 17500 \text{ K}$  for  $\epsilon$  Eri b and  $\sim 15250 \text{ K}$  for 55 Cnc d. Then the acceleration of gravity ( $g$ ) and the mean density ( $\langle \rho \rangle$ ) are derived. Their values are given in Table 4.

Planet	$R_p$ ( $R_J$ )	$g$ ( $\text{m/s}^2$ )	$\langle \rho \rangle$ ( $\text{gr/cm}^3$ )	$D$ ( $\text{H}_2$ ) ( $R_p$ )
$\epsilon$ Eri b	1.1	23	0.9	0.09
55 Cnc d	1.05	208	10	0.03
Jupiter	1	23	1.33	0.15

Table 4. Structure data.

In Figure 1 we present the thermal structure in the upper atmosphere “the troposphere” (up to  $P \sim 20 \text{ bar}$ ) based on a radiative – convective equilibrium model that uses for the radiative part the Milne - Eddington approximation and an adiabatic profile for the convective part. The tropopause level where  $dT/dz = 0$  is defined by  $T_{\text{trop}} = (5/4)^{1/4} T_{\text{eff}}$  and  $P_{\text{trop}} = 1.6 (g/K_R)$  where the mean Rosseland opacities ( $K_R$ ) are taken from Ref. [13]. Figure 1 also traces the saturation vapor pressure curves for a solar composition of ammonia and water, the two most plausible condensables to form clouds in such planets. Note that  $\epsilon$  Eri b could have water clouds in the troposphere ( $P \sim 0.5 \text{ bar}$ ) with their base changing in altitude with the seasonal cycle. Water clouds are known to be very active in producing horizontally large wet convective storms in Jupiter [14-15] and in Saturn [16-17]. Thus this planet could show stormy activity that can manifest as bright spots in its disk as occurs in Jupiter and Saturn. On the contrary, no massive clouds are expected in the troposphere of 55 Cnc d. The reflectivity of the planet should be dominated by Rayleigh scattering in the dense gaseous atmosphere (Rayleigh scattering unit optical depths are reached at  $\sim 40 \text{ bar}$  for a wavelength of  $500 \text{ nm}$ ) or by the plausible presence of high altitude hazes forming close to the tropopause as occurs in the Solar System

giants. In Table 5 additional thermal structure data are presented: for these planets at the tropopause level: the atmospheric scale height  $H = R_g T / \rho g$  is the e-folding vertical scale for pressure ( $R_g$  is the gas constant), the adiabatic gradient  $G_{adiab} = g/C_p$  ( $C_p$  is the specific heat at constant pressure), and the Brunt-Väisälä frequency given at the tropopause level ( $dT/dz=0$ ) by

$$N_{trop} = \frac{g}{\sqrt{C_p T_{trop}}} \quad (3)$$

It is an index that represents the stability of the atmosphere to vertical motions and is also a parameter that controls the scale of horizontal motions in a baroclinic atmosphere (see section 6 and [18]).

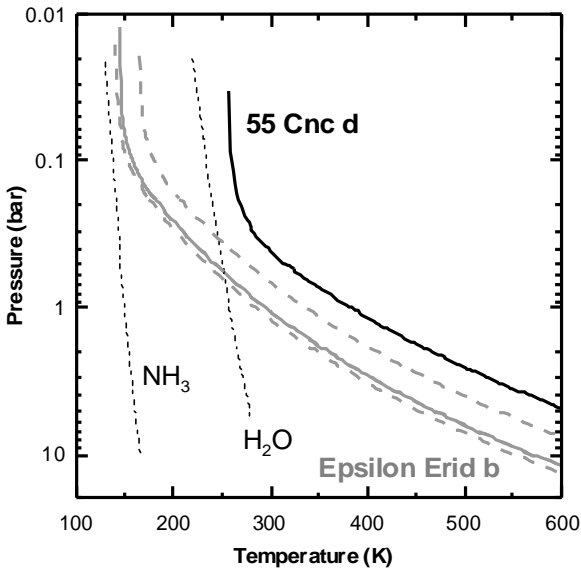


Fig. 1. Temperature - Pressure mean vertical profiles in the atmospheres of  $\epsilon$  Eridani b and 55 Cancri d (continuous lines). The dashed lines for  $\epsilon$  Eridani b shows the extreme profiles expected for periastron and apoastron distances of the planet to the star. The saturation vapor pressure curves for a Jovian composition of ammonia and water are also shown. The intersection of these curves with the atmospheric profiles, mark the points where the cloud base forms.

Planet	$T_{trop}$ (K)	$P_{trop}$ (bar)	$H$ (km)	$G_{adiab}$ (K/km)	$N_{trop}$ ( $s^{-1}$ )
$\epsilon$ Eri b	181	0.18	30	1.3	0.15
55 Cnc d	323	0.55	6	16	0.1
Jupiter	113	0.1	19	2	0.02

Table 5. Temperature and vertical stability data.

## 5. ON THE ROTATION PERIOD

Rotation is the basic ingredient in atmospheric dynamics. All the Solar System planets with substantial

atmospheres have on the average their motions directed zonally (i. e. East-West) independently of: (a) the rotation angular speed (ranging from 243 days in Venus to 10 hr in Jupiter), (b) the intensity of the thermal energy sources (changing by a factor  $\sim 1730$  from Venus to Neptune), and (c) the spin axis tilt with respect to the orbital plane (the most extreme case is Uranus that has a tilt of  $90^\circ$ , but with zonal motions instead of pole - equator motions as should be expected if driven solely by heat transfer from the hottest to coolest points in the planet). Meridional (i. e. North - South) motions are of course present in these atmospheres (e. g. Hadley cells in Venus, Earth and Mars, and suspected in the giants) and in some cases they could be coupled to the zonal motions.

The rotation angular speed is thus a fundamental parameter for atmospheric dynamics. A main problem is that it is unknown for extrasolar planets, although it can be constrained by possible formation scenarios and assuming they do not have a massive satellite that could spin-up or spin-down the planet along its history. First, the minimum rotation period (the highest angular speed) the planet can reach is limited to the planet disruption by centrifugal forces, and is given by

$$t(\text{min}) = 2p \sqrt{\frac{R_p}{GM_p}} \quad (4)$$

Second, empirical relationships (rotation period with radius and mass) found for the Solar System giants can be used as a reference. Apparently, there is a convergence behavior toward the 10 hr rotation period in these relationships as one approaches the mass and radius of Jupiter. Third, numerical simulations of giant planet formation in gravitationally unstable disks show the first stages of planet formation with gravitationally self-bound rotating planets. When contracting them to the mean density of Jupiter and assuming conservation of angular momentum periods for the final planets range from 3 to 35 hr [19].

We show in Figure 2 the most plausible range of values for the rotation period of these planets. We also include here the curve of the rotation period as a function of the planetary radius for a Jovian-like planet as it contracts during its history to the actual Jupiter radius through angular momentum conservation. From this analysis, we conclude that the most reasonable rotation periods for Jupiter-like planets at large distances of the star drop in the range  $\sim 5$  hr to 15 hr. We adopt here a rotation period  $t(\text{rot}) = 10$  hr similar to Jupiter and Saturn. Magnetic field coupling of the forming planet with its disk and gravitationally interaction with the spiral arms that feed it may de-spin partially the planet but this question remains largely unknown. It is evident that formation models of the giant planets can in the future give more precise values depending on the disk

properties. But again we should be able first to converge to a unique model of formation and reproduce the actual spin of the Solar System planets.

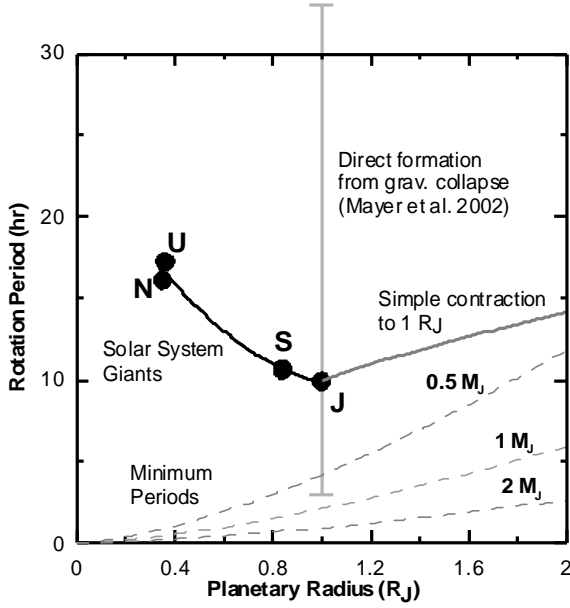


Fig. 2. Rotation period as a function of the planetary radius for several cases. Solar system giants (marked as: J = Jupiter, S = Saturn, U = Uranus, N = Neptune). Minimum rotation periods for different planetary masses due to the rupture by the centrifugal forces are indicated for different masses. A range of values according to formation model is shown as a vertical line [19]. A calculation from a simple contraction model of a Jovian-like planet to Jupiter radius using angular momentum conservation is also shown.

## 6. ATMOSPHERIC DYNAMICS: WIND SPEEDS

There are basically two main hypothesis to explain the alternating pattern of zonal (East-West) jets and banding in the giant planets Jupiter and Saturn [1]. In the “shallow layer” models the motions are confined to the upper troposphere (few bars), and are basically driven by the solar heating source and its differential deposition with latitude. In the “deep layer models” the motions extend along the molecular hydrogen layer (thousands of kilometers), and are basically driven by the internal heat source through convective transport that organizes the motions in columnar rotating cells that forms a system of counterrotating cylinders parallel to the spin axis. Because of the strong internal heating source in  $\epsilon$  Eri b and 55 Cnc d ( $\langle E \rangle \sim 7 - 135$ ), the horizontal (and in particular the meridional) temperature differences induced by insolation are expected to be low in the troposphere [20]. The stellar irradiation source could play a significant role only in the upper atmospheric levels above clouds, but here we assume

the motions to be primarily driven by the internal heat source since as indicated  $E \gg 1$ .

The first natural constraint to the atmospheric wind velocities comes from the sound speed in the troposphere:

$$c_s = \sqrt{g H} \quad (5)$$

being  $g = 1.4$  the adiabatic coefficient. On the other hand, convective motions are expected to be intense (Rayleigh number well above the critical one), with vertical velocities given, according to the mixing length theory [21], by

$$w = \left[ \frac{R_g}{m} \frac{F_{\text{int}}}{r C_p} \right]^{1/3} \quad (6)$$

For the above assumed rotation period, the strong convective motions in the  $H_2$  layer could be organized in a system of zonal jets [22], although the development of the counterrotating cylinders will be strongly constrained by the thickness of the  $H_2$  layer. This layer can be considered as “shallow” (compared to the planetary radius) in the case of  $\epsilon$  Erid b and 55 Cnc d (and actually even in Jupiter), so it is not evident that the cylinders system can develop. However the Rossby number  $Ro$  (a ratio between the wind relative to Coriolis accelerations),

$$Ro = \frac{u}{f L} \quad (7)$$

when approached to a limiting value  $Ro(\text{lim})$

$$Ro(\text{lim}) \approx \frac{c_s}{R_p \Omega} \quad (8)$$

is  $\leq 1$  (Table 6). Here  $u$  is the zonal wind velocity,  $L$  a characteristic horizontal length scale and  $f = 2W \sin j$  is the Coriolis parameter, with  $j$  the latitude. Coriolis forces will dominate and drive the system to two-dimensional (horizontal) motions, and thus geostrophic conditions are expected [18], with zonal (East-West) motions developing in the atmospheres of  $\epsilon$  Eri b and 55 Cnc d (as we see in the Solar System giants). However, if we similarly define a vertical Rossby number [2] we get,  $Ro(\text{vert}) \sim w/WH \sim 3$  for  $\epsilon$  Erid b and  $\sim 30$  for 55 Cnc d. This means that the internal energy source could produce intense enough vertical motions that could overcome Coriolis accelerations, making the motions more tri-dimensional in nature (with cellular patterns extending horizontally a scale  $\sim H$ ) favoured in the equatorial latitudes where the Coriolis force becomes

low. Concerning the zonal velocities, we can bound them using the following constraints:

a) As an upper limit we can take the sound speed given by (5), and assume that maximum wind speeds should be  $u(\max) \sim c_s$ .

b) For rapidly rotating systems under the geostrophic approach, the development of two-dimensional motions requires the Richardson number, defined as

$$Ri = \frac{N^2}{du^2/dz^2} \quad (9)$$

to be  $Ri < 0.25$  in order to prevent the growth of Kelvin-Helmholtz instabilities [21]. Here  $z$  is the vertical coordinate. Note that if vertical (convective) motions dominate, then  $N^2 < 0$  and  $Ri < 0$ . An order of the magnitude for the maximum horizontal wind speeds based on the Richardson constraint can be derived assuming that the vertical sheared motions extend over an scale height ( $H$ ), so  $u(\max Ri) \sim 2 N_{trop} H$ , where we take  $N_{trop}$  as given by eq. (3). Note that if the vertically sheared motions extends much deeper (for example along the whole  $H_2$  layer with thickness  $D$ ) the winds should be similar since  $N(z)$  depends on altitude and tends to zero with depth as the layer becomes more convective.

c) As a third approach we can use the Rossby number limit of 0.1 previously derived, and apply eq. (7) re-scaling it for motions of different length-scale. For example we can assume the horizontal length scale  $L$  to be of the order of the thickness of the  $H_2$  layer (vertical extent  $D$ ). Then for  $Ro \sim 0.1$ , we re-scale the zonal wind velocity to  $u(Ro) \sim Ro \ 2W \ D$ . The range of wind velocities, including the Rossby number estimate, is presented in Table 6.

Planet	w (m/s)	$c_s$ (m/s)	Ro	u(max Ri) (m/s)	u(Ro) (m/s)
$\epsilon$ Eri b	16	980	0.07	900	170
55 Cnc d	32	1320	0.1	1200	80

Table 6. Wind velocities.

## 7. ATMOSPHERIC DYNAMICS: SPATIAL AND TEMPORAL SCALES

### 7.1 Meridional scale and number of jets

Under geostrophic conditions, the meridional gradient of the Coriolis force  $\mathbf{b} = df/dy$ , two-dimensional turbulence dominates and drive the zonal motions toward a pattern of jet, alternating their direction with latitude, and establishing a “differential rotation”

between latitudes [1] with the meridional jet width scaled by the Rhines length  $L_b$

$$L_b = \sqrt{\frac{u}{b}}, \quad \mathbf{b} = \frac{2\Omega \cos j}{R_p} \quad (10)$$

The number of expected jets per hemisphere is then:

$$n \approx \frac{p R_p}{2 L_b} \quad (11)$$

### 7.2. “Spot” scales

Under geostrophic conditions, a natural horizontal length scale for mid-latitude disturbances (vortices and waves), is given by the Rossby deformation radius  $L_D$

$$L_D = \left( \frac{NH}{f} \right) \approx \frac{N_{trop} H}{\Omega} \quad (12)$$

Observations of the giant planets features suggest however, that these spots and disturbances have typically horizontal scales  $L \sim 10 L_D$ . Meteorological features will appear, if traced by the clouds, as contrasted “spots” in the planetary disk. The contrast will depend on the altitude differences for these features above or below the cloud deck, or in the presence within the spots of particles of different composition or sizes, so their scattering properties becomes different to those of the cloud deck. In Table 7 we give an estimate of the characteristic values for the horizontal in both planets.

Planet	$L_b$ (km)	n	$L_D$ (km)	10 x $L_D$ (km)
$\epsilon$ Eri b	27000	4-5	2500	25000
55 Cnc d	18800	6	3400	34000

Table 7. Jets and horizontal scales of motion.

The rotation period of the features moving with velocity  $u$  relative to the intrinsic (internal) rotation period of the planet (adopted here to be  $t_{rot} = 10$  hr) is

$$t_{feature} = \frac{2pR_p t_{rot}}{u t_{rot} + 2pR_p} \quad (13)$$

Assuming the features to move with our adopted maximum wind speed ( $u = \pm c_s$  + eastward, - westward) gives a rotation period in the range  $t_{feature} \sim 9.25$  hr to 10.75 hr. Much larger differences should be however found if the planet rotates slowly and the zonal winds are intense, as occurs for example in Venus whose atmosphere is superrotating (4 day period) although the rotation period of the planet is slow (243 days). If direct detection of these planets is reached, photometric variability produced by the spots could be

used to constraint the atmospheric rotation period, but unfortunately no the intrinsic rotation period of the planet since this should be derived, as in the solar system giant planets, from the rotation of the magnetic field (radio variability).

### 7.3 Temporal scales

The relevant temporal scales are the spin period (adopted 10 hr), the orbital period ( $t_{orb}$ ), the radiative time constant period, that is the time for temperature changes due to heating source changes,

$$t_{rad} = \frac{C_p P_{trop}}{4s g T_{trop}^3} \quad (14)$$

being  $s$  is the Stephan-Boltzman constant. The dynamical time constants are the horizontal ( $t_{dyn,h} = 2pR_p/c_s$ ) for zonal motions, and the vertical ( $t_{dyn,v} = H/w$ ) for convective motions. In Table 8 we summarize the values for these scales.

Planet	$t_{orb}$	$t_{rad}$	$t_{dyn,h}$	$t_{dyn,v}$
$\epsilon$ Eri b	6.85 y	1 y	4.1 d	0.5 d
55 Cnc d	14.7 y	21 days	2.9 d	0.05 d

Table 8: Temporal scales of motion

Two conclusions can be extracted from these numbers. First, from the ratio  $Go = t_{dyn,h}/t_{rad}$  (Golitsyn number) [2], we find that for both planets we have  $Go \ll 1$ . This means that the tropospheres of  $\epsilon$  Eri b and 55 Cnc d are far from radiative equilibrium, with their average thermal structure being governed by dynamics. This should be considered in future advanced models of cloud formation and albedo determination [11]. Second, since  $t_{rad}/t_{orb} < 1$ , seasonal changes can be expected in the upper part of the atmosphere where radiation dominates. In particular, because of its high eccentricity and short radiative time response, the planet  $\epsilon$  Eri b could suffer important seasonal changes in its general circulation above clouds where radiative transfer should dominate. The ratio of the stellar flux absorbed by the planet between the periastron and the apoastron is

$$\frac{F_{abs}(periastron)}{F_{abs}(apoastron)} = \frac{41.6}{2.6} \sim 16 \quad (15)$$

As a consequence the number  $E$  characterizing the dynamical regimen of  $\epsilon$  Eri b changes from 2 to 17 (if a constant mean albedo  $A = 0.4$  is assumed) or from 4 to 52 (for a constant mean albedo  $A = 0.8$ ), between periastron and apoastron. This planet could exhibit strong changes in the dynamical modes in its troposphere as the importance of the dominating source of energy (the internal heat flux) decreases as the planet

approaches periastron and the stellar irradiation becomes important. In this framework  $\epsilon$  Eri b could be regarded as a very interesting planet that could serve to test the opposed models so far developed to explain the general circulation in Jovian-like giants.

### Acknowledgements

This work has been supported by the MCYT Plan Nacional de Astronomía y Astrofísica 2000-0932 and by Grupos UPV-EHU 13697/2001. RH acknowledges a post-doctoral PhD fellowship from Gobierno Vasco.

### References

1. Ingersoll, *Science*, **248**, 308-315, 1990.
2. A. Sanchez-Lavega, *Astron. Astrophys.*, **377**, 354-360, 2001.
3. A. Sanchez-lavega, *Highlights in Spanish Astrophysics III*, Kluwer (in the press, 2003).
4. Showman A. and Guillot T., *Astron. Astrophys.* **385**, 166-180, 2002.
5. Menou K., et al., *Astrophys. J. Lett.*, **587**, L113-L116, 2003.
6. Cho J. et al., *Astrophys. J. Lett.*, **587**, L117-L120, 2003.
7. Schneider J. “*The Extrasolar Planet Encyclopaedia*”: <http://www.obspm.fr/encycl/encycl.html> and references therein.
8. Hatzes A. et al., *Astrophys. J. Lett.*, **544**, L145-L148, 2000.
9. Marcy G. et al., *Astrophys. J.*, **581**, 1375-1388, 2002.
10. Gatewood G., *Bull. Amer. Astron. Soc.*, **32**, 1051-1052, 2000.
11. Sudarsky D. et al., *Astrophys. J.*, **538**, 885-903, 2000, and astro-ph/0210216.
12. Burrows A. et al., *Astrophys. J.*, **491**, 856-875, 1997.
13. Guillot T., *Planet. Space Sci.*, **47**, 1183 - 1200, 1999.
14. Hueso R., and Sanchez-Lavega A., *Icarus*, **151**, 257-274, 2001.
15. Hueso R. et al., *J. Geophys. Res.*, **107**, 5/1-5/11, 2003.
16. Sanchez-Lavega A., et al., *Nature*, **353**, 397-401, 1991.
17. Sanchez-Navega A. et al., *Science*, **271**, 631-634, 1996.
18. Holton, J. R., *An Introduction to Dynamical Meteorology*, Academic Press, San Diego, 1992.
19. Mayer L. et al., *Science*, **298**, 1756-1759, 2002, and private communication.
20. Ingersoll A. P. and Porco C., *Icarus*, **35**, 27 - 43, 1978.
21. Stone P. H., in *Jupiter*, pag 586, T. Gehrels (ed), University of Arizona Press, Tucson, 1976.
22. Busse F. H., *Icarus*, **29**, 255 - 260, 1976.